NUMERICAL MODELING OF ATMOSPHERIC BOUNDARY LAYER CONDITIONS FOR A SCALED-DWON, LOW-SPEED WIND TUNNEL

Sheilla Torres-Nieves
Department of Mechanical Engineering
University of Puerto Rico at Mayagüez
PO Box 9000, Mayagüez, Puerto Rico 00681
sheilla.torres@upr.edu

Francesco Forina
Department of Mechanical Engineering
University of Puerto Rico at Mayagüez
PO Box 9000, Mayagüez, Puerto Rico 00681
francesco.forina@upr.edu

ABSTRACT

Atmospheric conditions occurring up to 1 km above the surface of the Earth are largely dominated by what is known as the atmospheric turbulent boundary layer. Understanding the atmospheric turbulent boundary layer is of great interest for many fields of study and industries. This investigation intends to numerically simulate the atmospheric turbulent boundary layer to accurately recreate these inflow conditions inside of a low-speed wind tunnel, guiding the experimental design to significantly reduce the number of design iterations and, hence, expedite the experimental setup time. To simulate realistic atmospheric conditions, including the atmospheric boundary layer profile, triangular vortex generators, called spires, were added to condition the incoming flow. The design of these spires was based on a methodology which uses the dimensions of the wind tunnel, the desired Hellman exponent and desired boundary layer height to generate the dimensions of the spire. Computational Fluid Dynamics simulations, using the commercial software Star CCM+, were performed to characterize the flow behavior generated by the spires. For this investigation, the ASCE (American Society of Civil Engineers) 7-16 classification for terrain types was used as the standard to compare the empirical data with acquired numerical results. According to the numerical results the Irwin design methodology overestimates the desired Hellman exponent to an average value of 17%, and it is recommended to start with the spire design process with a lower Hellman exponent than the intended design. The turbulence intensity profile showed some disagreement with past data of ASCE 7-16 which could be due to the lack of surface roughness on the bottom floor where the spires are present. More flow blockage devices could be added to induce roughness such as blocks or walls to induce a higher degree of turbulence to match the theoretical turbulence profile.

INTRODUCTION

The atmospheric boundary layer (ABL) is a region that exists between the surface of the Earth and the free atmosphere, both of which comprise the troposphere (Arya, 1988). This boundary is heavily influenced by the Earth's surface, particularly by its energy and moisture content (Oke, 1987), and its effects must be taken into consideration for applications such as structural purposes in the design of high-rise buildings, pollutant dispersion in cities or in the design of wind turbines, among others.

Turbulence plays a pivotal role in the definition of the structure of the atmospheric boundary layer (ABL). The ABL is nearly always turbulent (Tennekes, 1987) and it is this turbulence the most important transport phenomenon (Arya, 1988). In fact, it is the turbulent transport of heat of the atmospheric boundary layer that enables the uniformization of temperature of the Earth. However, turbulence adds complexity in the modeling or prediction of the ABL.

The diurnal and nocturnal periods, together with certain atmospheric conditions, affect the stability of the ABL. The stability of the ABL refers to the amount of turbulent kinetic energy being generated or subtracted due to buoyancy effects. During daytime (diurnal cycle), the sun heats the surface of the Earth which in turn heats the air, thereby creating eddies that extend throughout the boundary layer. When there is generation of turbulent kinetic of energy due to the heating of the surface, the ABL is classified as an unstable ABL. During the night, the ABL reduces in height since there is no generation of turbulent kinetic energy and the air suppresses any generation of turbulence due to buoyancy effects. This nocturnal behavior is labeled as a stable ABL. In neutral stable flows there is no generation or reduction of turbulent kinetic energy due to buoyancy effects; this behavior is classified as a neutrally stable ABL (ESDU, 1974). Neutrally stable atmospheric boundary layers can be seen in nature during overcast skies (complete cloud cover) (Arya, 1988) or during strong geostrophic winds.

As a boundary, it is modeled by equations that describe the variation of velocity as a function of height. The mean velocity gradient of turbulent boundary layers for smooth flat plates are normally modeled by the 1/7th power law (Schlichting, 1955). To better describe the turbulent mean velocity profile of the ABL,

$$\frac{u}{U_{ref}} = \left(\frac{\mathrm{y}}{\mathrm{y_{ref}}}\right)^{\mathrm{m}}$$

where u is the velocity at a vertical distance y, $yref$ is a reference height and $Uref$ refers to the velocity of the wind at a height of 10 meters (standard height of elevation for measurement with anemometers to reduce interference with surface features) (Hellmann, 1917). The exponent m is the Hellmann exponent, and it is a function of the roughness features of the surface of the Earth and the stability of the ABL (i.e., stable, neutrally stable, or unstable).

The values of different Hellmann exponents depend on the type of terrain. As the terrain has more roughness, the

Hellmann exponent increases. According to ASCE 7-16 (American Society of Civil Engineers) the terrain is classified as types A, B, C and D, arranged from roughest terrain setting to smoothest. For instance, D terrain corresponds to calm water or open seas, and have a Hellmann exponent of 0.12, whereas an A terrain with regular, large obstacle coverage has a Hellmann exponent of 0.33.

Normally, a neutrally stable ABL is recreated at laboratory scale in wind tunnels. These are called "Boundary Layer Wind Tunnels" (BLWTs) but are too large and not always available for researchers (Dommelen, 2013). Moreover, the high cost of renting a large-scale private wind tunnel might be prohibitive. Smaller scale wind tunnels that are not specifically designed to simulate ABLs inlet are adapted with the addition of flow blockage devices or vortex generators to mimic the ABL flow characteristics by transforming the uniform laminar velocity into a turbulent velocity gradient downstream. These vortex generators can be triangular such as spires or can have distinct profiles to force a specific velocity gradient downstream. However, the design of these devices is largely based on a highly iterative process which is typically time consuming.

Another way to simulate the atmospheric boundary layer is by using numerical methods using Computational Fluid Dynamics (CFD). The application of CFD in the study of ABL is still the subject of research to this day, since it has reaped benefits in the understanding of this complex flow phenomenon, and it also has helped in the development of wind tunnels specialized in recreating the ABL. CFD models validated by experimental results can help reduce the reliance on wind tunnels, thereby providing a more cost-effective method.

The main objective of this study was to design spires by using a commercially available flow solver (Star CCM+) to simulate the ABL flow conditions in a virtual wind tunnel and to use RANS turbulence models, such as k-epsilon and SST k-omega, as part of the design. This is intended to guide the experimental design to adapt a small-scale wind tunnel for ABL testing capabilities, significantly reducing the number of design iterations and, hence, expediting the experimental setup time. The validated numerical simulation will be used to study phenomenon such as modeling pollutant dispersion in cities in Puerto Rico and for scaled-down wind turbine design.

NUMERICAL MODELING

The main objective of this investigation is to numerically simulate a neutral atmospheric boundary layer in a virtual wind tunnel. Specifically, this numerical investigation intends to recreate a type D terrain specification according to ASCE 7-16 which pertains to a boundary layer with open seas characteristics and has a Hellmann exponent of 0.12. For instance, this could allow the study of offshore wind farms off the coast of Puerto Rico to provide electricity to the island. Numerical simulations were performed to realistically model the experiments to be performed in a small-scale low-speed wind tunnel. Hence, the dimensions of the numerical model are based off the dimensions of the wind tunnel test section (150 mm x 150 mm x 455 mm).

The boundary conditions of the simulation are a velocity inlet condition with a constant 10 m/s velocity profile entering the domain, a pressure outlet aft of the simulation, wall conditions on the upper and lower boundaries and symmetry planes on the lateral sides of the boundary. The physical models used are a steady state, constant density model, segregated flow. The turbulence model chosen for the simulation is the k-omega SST model. This model has been used in other studies (Shojaee et al. (2013), Abubaker et al. (2018) and Hobson-Dupont (2015)) to numerically recreate the ABL in a virtual wind tunnel and has been known to work for separated flows. The inlet conditions of the simulation also include a 1% turbulence intensity (the measured value for the inlet condition for the wind tunnel) and a turbulent length scale of 7% of the spire height.

Spire Design

To recreate the ABL profile, triangular flow blocking devices or spires were added at the entrance of the domain. The dimensions of these spires were based on Irwin's design methodology (1981). A desired boundary layer height of 70 mm was established preliminarily based on the models to be tested in the wind tunnel. With a Hellmann exponent of 0.12, akin to the surface roughness of open flat terrain or offshore wind farms (D terrain type), and the wind tunnel height of 150 mm the dimensions of the spire were calculated from the empirical relations (Irwin, 1981). The spire height was calculated to be 91.7 mm, but the height was reduced to 84 mm due to the addition of a rounded edge for meshing purposes. The spacing between spires was calculated to be half of the intended spire height (91.7mm) and the length of the triangular splitter plate in the back of the spire was calculated to be a quarter of the spire height. The height of the splitter plate set as half of the spire height. Lastly, the thickness of the spire is 1 mm. Figure 1 provides a schematic and additional details on the spire geometry.

Domain

The height and width of the virtual wind tunnel have the same values of the real model, but the overall length of the test section was increased to study the effect of flow development. The distance between the velocity inlet and the spire was made up to be roughly two spire heights to avoid convergence issues due to backflow. The velocity measurements of the simulation will be taken at different locations downstream, from one to six spire heights in length, to see where the flow becomes fully developed. Velocity profiles will be compared with the power law to verify if the spire provides the required momentum deficit to recreate the ABL downstream. The interrogation locations of these velocity profiles and the overall length of the domain is depicted in figure 2.

Meshing

A polyhedral mesh was used to capture the bulk flow of the simulation and prism layers were added to solve for the viscous sublayer of the wall of the spires and the wall. The advancing layer mesher was used to reduce the distortion of the grid at right angles. Also, the tip of the spire was rounded to save computational resources. Figure 3 shows the transverse view of the mesh and details of the mesh at the spire tip. As shown in figure 3a, the mesh is finely defined at the tip of the spire to provide a mesh that adequately captures the geometry of the tip. The surface growth rate is 1.05 to provide a smoother transition between the mesh of the surface and the mesh of the overall volume. Three prism layers were added to capture the viscous sublayer of the surface of the spire, but the mesh was constructed with the intention to capture the gross flow features of the flow volume.

The Irwin design method provides a basis for the first design iteration. To ensure that the simulation is providing valid results with the first design iteration a mesh sensitivity study was performed. The basis for the mesh sensitivity study was to identify how many elements are required for the velocity profile at 6 spire heights to be independent of the mesh. The surface grid was refined from 670 thousand elements to 2.7 million elements to verify mesh independence based on velocity profile changes. According to the mesh sensitivity study the velocity profile at 6 spire heights stabilized at one million elements by reducing the surface size of the mesh at the spire. The mesh parameters for the subsequent simulations were based on the 2 million count to guarantee convergence for any possible case.

To ensure convergence, several monitors were placed at 6 spire heights length downstream and at 8 positions above the wall from 5 mm to 75 mm in height to verify if the velocity achieved convergence. Another convergence criterion was a mass flow average monitor plot at the outlet of the domain (Hubson-Dupont, 2015). Monitors of both plots showed that convergence was achieved after 300 iterations.

Spire design normally entails an iterative process. However, by comparing numerical simulations with experiments, the number of iterations can be drastically reduced. For the first run, the spire array will provide a velocity gradient downstream which is compared to the theoretical velocity profile given by the power law. If there is any discrepancy between the measured and the theoretical profiles, dimensions of the spire will be changed. The tests will be repeated until the desired velocity profile downstream is achieved.

As part of this study, numerical runs were performed to understand how the Irwin methodology responds to the desired power law at 6 spire heights. The desired boundary layer height and Hellman exponent were varied. The turbulence intensity was also varied to match turbulence intensity of the ABL according to Garratt (2002). A parametric study consisting of 12 numerical simulations was conducted to study the impact of varying the desired boundary layer height, turbulence intensity, Hellman exponent, and spire geometry. The domain was interrogated at different locations downstream, from one to six spire heights in length, to identify when the flow is fully developed. The acquired velocity profile was compared with the power law to verify if the spire provided the required momentum deficit to recreate the ABL downstream. Table 2 details the case matrix for this study.

RESULTS AND DISCUSSION

According to Irwin's design methodology and the results of Shojaee et al. (2013) for a smooth wall the desired velocity profile is achieved at a length equivalent of six spire heights downstream. In this case, the desired boundary was outside the available test section (about five spire heights). Figure 4 shows that the flow is fully developed after 5 spire heights.

The velocity contours of the spires show that the wake of the spire is still present at less than one spire height downstream and the velocity gradient normal to the wall has a smoother profile after some distance from the spire. As expected, it is observed that the flow compensates the velocity deficit caused by the spire by accelerating the flow upwards and thereby, creating an equivalent free stream velocity. The maximum velocity of 15 m/s occurs at the tip of the spire. The interaction between the spires was also investigated, as shown in figure 5a. The flow stabilizes at approximately 2 spire heights downstream from the spire but in the immediate vicinity of the spire the middle spire tends to vortex shed. These instabilities are not present downstream, after 2 spire heights. It was also observed that the wake of the spire extended up to one spire height downstream. Another observation is that the flow was laterally symmetric which is consistent with the results of Shojaee et al. (2013).

The further validate the simulation, the velocity profile at six spire heights was fitted with the power law (figure 5b) to determine the Hellman Exponent and was normalized with the free stream velocity. In this case the boundary layer and the free stream velocity at six spire heights were 61.0 mm and 10.83 m/s, respectively. Recall that the design was intended for a boundary layer height of 70 mm, showing good agreement with the numerical result. This difference is due to the acceleration of the flow in the upper portion of the tunnel which burrows into the decelerated flow caused by the blockage.

The power law in real scale is valid only from a reference height of 10 meters and above (Garrat, 2002). The full-scale height of the surface layer of the ABL in this case is 300 meters. The boundary layer calculated from the simulation was later scaled to identify the equivalent of 10 meters of the velocity profile in the simulation, which was calculated to be 0.002 meters. The power law was fitted starting from 0.002 meters to the height where the velocity normalizes to the boundary layer height. The Hellman exponent in this case was calculated to be 0.157, a 26% difference from the desired value of 0.12. The Irwin's design method overestimates the desired Hellman exponent in this case and so the study was extended to other designs of spires based on the same desired boundary layer height but of different Hellman exponents. The overestimation of the Hellman exponent of the simulation can be seen in a previous numerical investigation with spires by Hobson-Dupont (2015), with the difference being that the author also used roughness elements in the simulation.

Additional studies were conducted by changing the power law, desired boundary layer height and turbulence intensity. The first set of cases analyzed changes in the power law to account for the previously observed numerical overestimation of the Hellmann exponent. Case 2, for instance, used a Hellmann exponent of 0.09 to design the spires to analyze if the simulation would predict a power-law exponent closer to the intended 0.12. With an intended Hellman Exponent of .09 the height of the spire increased slightly to 93 mm compared with the previous iteration of 91 mm, but the base of the spire decreased from 7.4 mm to 6 mm. This results in a lower flow blockage compared with the previous spire design. In this case 2, the Hellmann exponent is calculated to be 0.135 which is close to the desired profile for the numerical investigation of 0.12 by an 11% difference, but the intended design was 0.09 which corresponds to a 40% difference. Case 3 was based on a Hellman exponent of 0.16; according to ASCE 7-16 this is equivalent to Type C terrain which is open terrain with few obstacles. Numerical results for case 3 matched the intended Hellman exponent. Hence, as shown in figure 6, at 5 spire heights the velocity profile in in agreement with the power law and, hence, this setup can be used to accurately simulate a Type C terrain, which according to ASCE 7-16 has a Hellmann exponent of 0.16.

The effect of turbulence intensity was also studied. For this, the turbulent intensity was increased to 10% which would allow the free stream turbulence to be akin to the atmospheric boundary layer. The turbulent intensity at the inlet for cases 1 to 6 was 1% which is the turbulent intensity of the experimental wind tunnel. Cases 1 to 6 with an increase

in turbulence intensity to 10% are defined as cases 7 to 12. For case 7 where a Hellman exponent of 0.12 and a 70 mm boundary layer height increasing turbulence intensity from 1% to 10% results in a Hellman exponent decreasing from 0.152 to 0.128 (30% decrease), which makes it more suitable to simulate Type D terrain. However, the boundary layer height increases from 65.7 mm to 75 mm which is closer to the desired boundary layer height. Figure 7a summarizes the results for cases ran with turbulence intensities of 1% (cases 1-3) and at 10% (cases 7-9). After comparing the simulations of 1% and 10% turbulence intensity it has been noticed that the Hellman exponents are lower for 10% than for 1% and the boundary layer thickness is greater for the 10% turbulence intensity. This was also confirmed by the results for the cases performed for a desired boundary layer thickness of 50mm. With this study it has been confirmed that by increasing the turbulent intensity profile the boundary layer thickens and the Hellman exponent decreases.

Another parameter used to confirm the presence of a scaled atmospheric boundary layer is the turbulent intensity profile of the ABL as defined by Zhou et. al (2002). The intent of this investigation is to provide a spire design that can generate a power law of 0.12 equivalent to terrain characteristics of Type D according to ASCE 7-16. The cases used for this study are cases 1 and 7, and the profile is at six spire heights. It can be seen in figure 7 that the empirical profile has more turbulent intensity than the simulation. The turbulence intensity was increased to 10% at the inlet and the turbulence intensity at the freestream increased from 0.7% to 5% but it did not match the desired overall profile. Roughness features such as blocks should be added at the floor to enhance turbulence close to the wall to better match the empirical profile. The addition of other flow blockage devices such as a small fence or chains (smaller than the height of the spire) together with the spire design could be used to provide more turbulence intensity. The spires alone are insufficient at providing the desired turbulent intensity profile and must be assisted with other means of turbulent generation.

CONCLUSIONS

The objective of this study was to provide a spire design that could replicate a Type D terrain with its characteristic velocity and turbulence profiles. The spire design was generated using the Irwin method which, according to the results, seems to generally overestimate the desired Hellman exponent. In this case it could be due to insufficient roughness on the bottom wall.

When the turbulence intensity at the inlet is increased, the boundary layer height increases on an average of 25%, and the Hellman exponent decreases on average by 15%. The boundary layer height increases due to the addition of turbulent energy at the inlet, which thickens the boundary layer. The addition of turbulence intensity at the inlet was implemented to match the desired theoretical turbulent intensity profile, but it is insufficient to adequately capture the theoretical power law. Roughness elements or a small wall could be added to increase the turbulence intensity close to the wall to match this profile.

Once a numerical simulation is validated for the design of spires for atmospheric boundary layer modeling, the design phase for an experimental setup could be significantly reduced from months to weeks. However, it is confirmed that additional elements might be needed to generate a profile that accurately resembles the atmospheric boundary layer. The spires alone are insufficient at providing the desired turbulent intensity profile and must be assisted with other means of turbulent generation.

REFERENCES

Abubaker, A., Kostić, I., Kostić, O., Stefanović, Z., 2018, “CFD modeling of atmospheric boundary layer simulations in wind tunnels”, *Tehnicki vjesnik - Technical Gazette*, *25*(6), pp. 1595-1598.

Arya, S. P., 1988, “Mean Boundary Layer Characteristics”. In *Introduction to Micrometeorology*, 1st ed., pp. 1-12.

ASCE, 2010, “Minimum design loads for buildings and other structures”, *ASCE 7-10*, Reston, VA.

Dommelen, R. V., 2013, “Design of an atmospheric boundary layer wind tunnel. Thesis / Dissertation ETD.

ESDU, 1974, “Characteristics of atmospheric turbulence near the ground”, *Engineering Science Data Unit*. Numbers, 74030 and 74031.

Garratt, J., 2002, “The Atmospheric Boundary Layer. *Cambridge Atmospheric and Space Science Series*.

Hellman, G., 1917, On the Motion of Air in the Lowest Layers in the Atmosphere. Meteorologische Zeitschrift, 34, 273.

Hobson-Dupont, M., 2015, *The Development of a Small Scale Wind Tunnel Simulating the Atmospheric Boundary Layer*, San Jose University.

Irwin, H. P. A. H., 1981, “The design of spires for wind simulation”, *Journal of Wind Engineering and Industrial Aerodynamics*, 7, pp. 361-366.

Oke, T.R., 1987, “Boundary Layer Climates”, Halsted Press, New York, NY, USA, 2nd edition.

Schilichting, H., 1955, “Boundary Layer Theory”, Pergamon Press: London; Verlag G. Braun: Karlsruhe.

Shojaee, S. M., Uzol, O., & Kurç, Ö., 2013, Atmospheric boundary layer simulation in a short wind tunnel, *International Journal of Environmental Science and Technology*, 11(1), pp. 59-68.

Tennekes, H., and Lumley, J. L., 1987, “A first course in turbulence”, Cambridge, MA: MIT Press.

Zhou Y., Kijewski T., Kareem A. (2002), Along-wind load effects on tall buildings: comparative study of major international codes and standards. Journal of structural engineering. 2002, 128(6):788-796

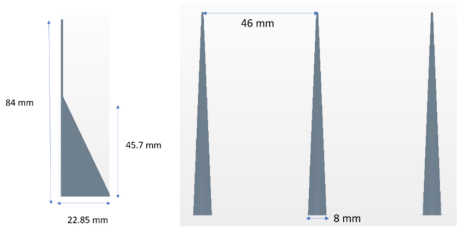

Number of Spires	3
Desired Boundary Layer Height	70.0 mm
Intended Height of Spire	91.7 mm
Height of Spire	84.0 mm
Base of Spire	8.00 mm
Base of Splitter	22.8mm
Height of Splitter	45.7 mm
Thickness of Spire	1.00 mm
Hellman Exponent	0.12

Figure 1. Spire; (a) geometry, and (b) dimensions.

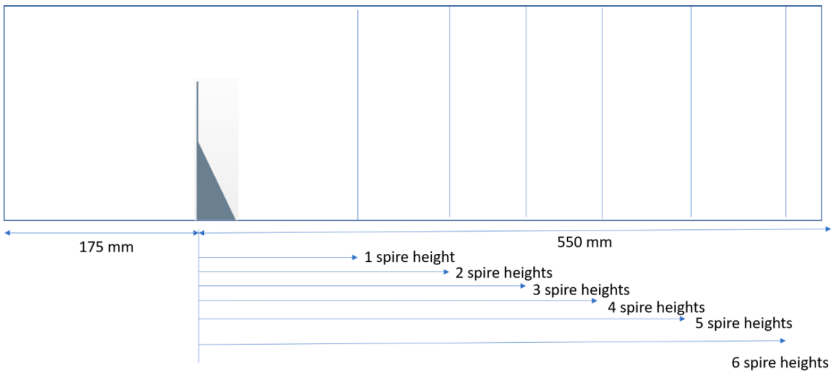

Figure 2. Selected interrogated locations and domain length.

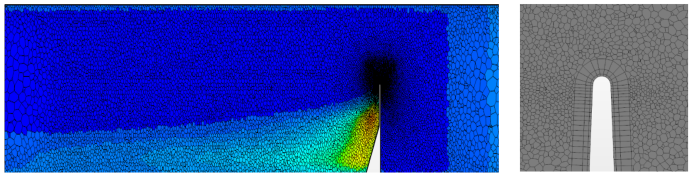

Figure 3. Mesh schematic, (a) mesh in computational domain, and (b) close-up near spire tip.

Case Number	Boundary Layer Height (mm)	Turbulence Intensity (%)	Hellman Exponent	Height (mm)	Base (mm)	Spacing (mm)
1	70.0	1.00	0.12	86.0	7.40	45.8
2	70.0	1.00	0.09	81.7	6.20	46.5
3	70.0	1.00	0.16	84.8	8.70	45.0
4	50.0	1.00	0.12	58.2	5.37	32.7
5	50.0	1.00	0.09	56.5	4.46	33.0
6	50.0	1.00	0.16	58.8	6.47	32.0
7	70.0	10.0	0.12	86.0	7.40	45.8
8	70.0	10.0	0.09	81.7	6.20	46.5
9	70.0	10.0	0.16	84.8	8.70	45.0
10	50.0	10.0	0.12	58.2	5.37	32.7
11	50.0	10.0	0.09	56.5	4.46	33.0
12	50.0	10.0	0.16	58.8	6.47	32.0

Table 2. Numerical simulations performed.

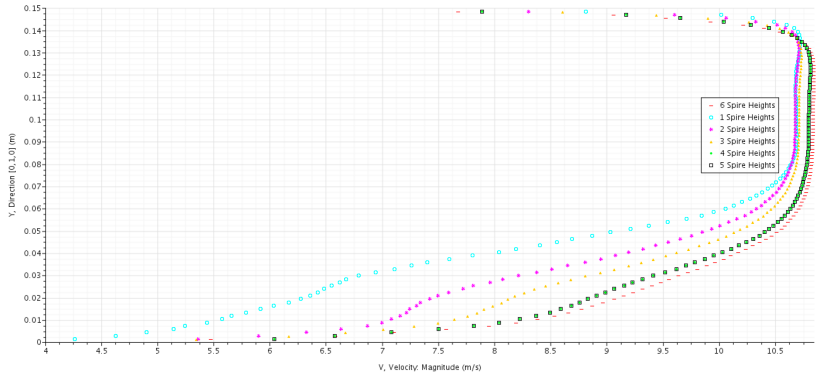

Figure 4. Velocity profiles showing fully developed flow location.

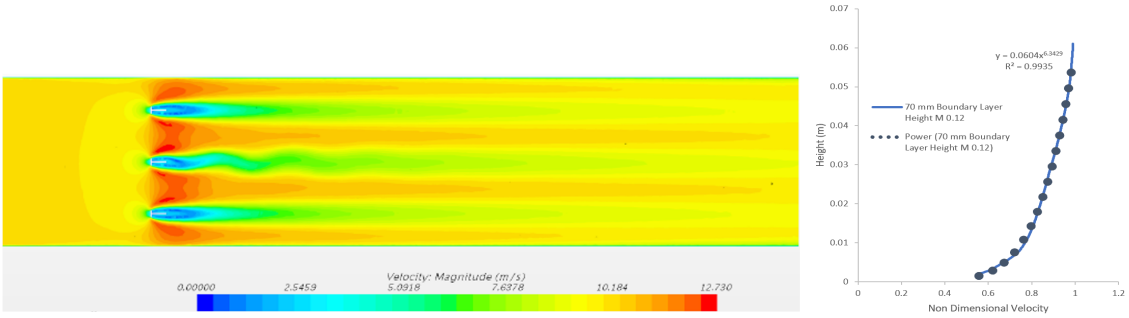

Figure 5. Case 1 velocity (a) velocity contours for top view at half spire height, and (b) velocity profile at a downstream location of six spire heights (fully developed)

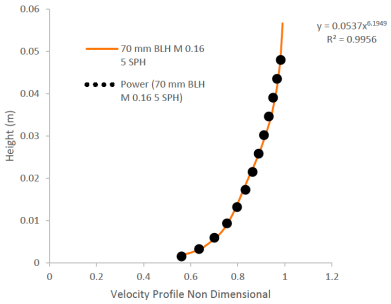

Figure 6. Velocity profile for Case 3 at a downstream location of six spire heights (fully developed)

Case Number	Boundary Layer Height (mm)	Turbulence Intensity (%)	Hellman Exponent	Numerical Hellman Exponent	Hellman Exponent Percent Difference (%)	Numerical Boundary Layer Height (mm)
1	70.0	1.00	0.12	0.157	26	65.7
2	70.0	1.00	0.09	0.135	40	61.0
3	70.0	1.00	0.16	0.161	0.6	57.4
7	70.0	10.0	0.12	0.128	6.4	75.0
8	70.0	10.0	0.09	0.117	26	72.7
9	70.0	10.0	0.16	0.140	13	74.0

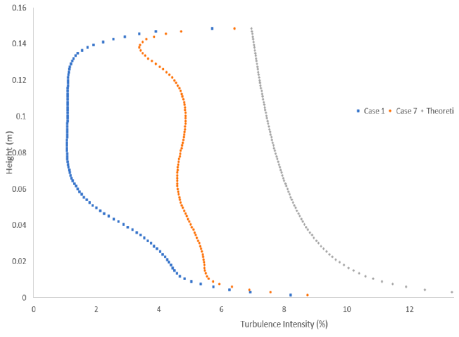

Figure 7. (a) Results for cases with 1% and 10% turbulence intensity for 70mm desired boundary layer height (b) turbulence intensity for cases 1 and 7